Journal of Magnetic Resonance 309 (2019) 106621

Contents lists available at ScienceDirect

Journal of Magnetic Resonance

journal homepage: www.elsevier.com/locate/jmr

Electron spin echo detection of stochastic molecular librations: Non-cooperative motions on solid surface

Elena A. Golysheva [a,b], Rimma I. Samoilova [a], Marta De Zotti [c], Claudio Toniolo [c,d], Fernando Formaggio [c,d], Sergei A. Dzuba [a,b,*]

[a] Institute of Chemical Kinetics and Combustion, Russian Academy of Sciences, Novosibirsk 630090, Russian Federation
[b] Department of Physics, Novosibirsk State University, Novosibirsk 630090, Russian Federation
[c] Department of Chemical Sciences, University of Padova, 35131 Padova, Italy
[d] Institute of Biomolecular Chemistry, Padova Unit, CNR, 35131 Padova, Italy

ARTICLE INFO

Article history:
Received 8 August 2019
Revised 12 October 2019
Accepted 12 October 2019
Available online 14 October 2019

Keywords:
Antibiotic peptide
Biological media
Cooperative motions
EPR
ESE
ESR
Glassy media
Neutron scattering
Spin label
Spin relaxation

ABSTRACT

In frozen biological media and molecular glasses only restricted motions exist; because of the weakness and disorder of intermolecular bonds these motions may have stochastic nature. Electron spin echo (ESE) spectroscopy of spin-labeled molecules allows detecting their restricted stochastic rotations (stochastic molecular librations). As in molecular disordered media motions may be highly cooperative, it would be desirable to investigate their spectroscopic manifestation also in the systems where cooperative effects would be certainly ruled out. In this work, ESE of spin-labeled molecules adsorbed on inorganic SiO_2 surface was investigated in a wide temperature range. The rate of motion-induced spin relaxation was found to become measurable above 130 K, increasing with temperature and attaining then a saturating behavior with a well-defined maximum near 250 K. For two types of molecules differing remarkably in their size and polarity (a small highly-polar nitroxide radical and a large spin-labeled peptide), quite similar results were obtained. This saturating behavior was quantitatively reproduced in simulations within a simple model of jump between two close orientations. Comparison with experiment allowed estimate that at 250 K the correlation time of the motion τ_c is of the order of several tens of nanoseconds and the angle α between two orientations is around 0.02 rad. As the found saturating behavior is a property of individual motions, for any other molecular system an excess of the spin relaxation rate above the maximum found here for adsorbed molecules may be ascribed to cooperative motions. Comparison with literature data on molecular systems of different origin has shown that effects of cooperativity indeed are present and, moreover, may be very essential.

1. Introduction

In solids at low temperatures, translations and rotations of atoms and molecules are suppressed, and only vibrations and restricted rotations of atomic groups and molecules (molecular librations) exist. In disordered molecular media, because of weakness and disorder of intermolecular interactions, vibrations and librations may have a stochastic (diffusive) nature. Stochastic molecular motions induce spin relaxation of spin labels which may be detected by electron spin echo (ESE) spectroscopy. This type of motion was detected by ESE in a large variety of molecular systems of different origin: molecular glasses [1–5], molecular crystals [3], frozen photosynthetic reaction centers [6–9], biological membranes [10–16], peptides and proteins [16–23], living seeds [24], polymers [25], frozen ionic liquids [26–28], and molecules confined in nanocapsules [29]. In these studies, the applicability of the theoretical librational model was quantitatively confirmed and relationships between dynamical and structural properties of the systems and their functionality were investigated.

Stochastic molecular librations are visible not only at the traditional X-band EPR, but at higher EPR bands as well [2,4–7,21,29–31]. At high-field W-band EPR, because of a higher sensitivity to the reorientations, also intramolecular motions (with the exception of molecular librations) may be detected [31]. In addition to the traditional nitroxide spin labels, also other types of spin-labeled systems were studied: quinone anions in photosynthetic reaction centers [6–8], triarylmethyl radicals [27], and transient triplet states appearing upon photoexcitation [32,33]. A librational

* Corresponding author at: Institute of Chemical Kinetics and Combustion, Ul. Institutskaya 3, 630090 Novosibirsk, Russian Federation.
E-mail address: dzuba@kinetics.nsc.ru (S.A. Dzuba).

https://doi.org/10.1016/j.jmr.2019.106621
1090-7807/

motion manifests itself also in continuous wave (CW) EPR [10,11,14–18,34–38] (note that CW EPR lineshapes are influenced also by conventional harmonic librations which do not result in spin relaxation).

In molecular media, stochastic molecular librations may appear not only because of an individual motion of a molecule in the cage formed by its surrounding but also because of a rearrangement of this cage. These cooperative motions of nearby molecules would result in appearance of motional hierarchy and different spin relaxation channels. To assess the possibility of motional cooperativity, it would be reasonable to investigate simpler systems in which cooperative effects certainly may be ruled out. Spin-labeled molecules adsorbed at low concentrations on solid inorganic surfaces presents a good example of such a system. Indeed, these surfaces do not participate in the motion, and low concentrations of spin-labeled molecules prevent mutual interaction between them.

In this work, we investigated in a wide temperature range stochastic molecular librations of spin-labeled molecules of two types – a relatively small nitroxide and a large spin-labeled peptide – which are adsorbed on an inorganic SiO_2 surface. The chemical structure of the nitroxide radical (NR) used in this work is shown below:

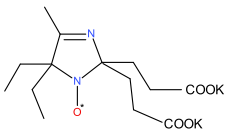

The amino acid sequence of the 10-mer spin-labeled peptide (TriTOAC4) is

*n*Oct-Aib-Gly-Leu-**TOAC**-Gly–Gly-Leu-Aib-Gly-Ile-Lol

where *n*Oct is *n*-octanoyl, Lol is the 1,2-amino alcohol leucinol, and the non-proteinogenic α-amino acids Aib (α-aminoisobutyric acid) and spin-labeled TOAC (2,2,6,6-tetramethylpiperidine-1-oxyl-4-amino-4-carboxylic acid) are

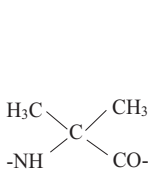

Aib

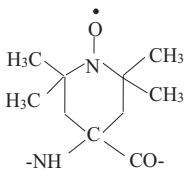

TOAC

This peptide is an analog of the antibiotic trichogin GA IV [39] in which Aib at position 4 is replaced by TOAC.

2. Experimental

2.1. Materials and methods

Pyrogenic silica powder was a commercial product from ZAO Polisorb, Chelyabinsk Region, RF (20 nm particle size, a specific surface area of 300 m^2/g). Nitroxide radical NR was kindly provided by Dr. I.A. Kirilyuk, Novosibirsk. Solid-phase synthesis, purification and chemical characterizations of the TOAC-labeled trichogin GA IV (TriTOAC4) sample used for spectroscopic measurements were carried out at the Department of Chemical Sciences, University of Padova, following our published procedure [39]. Electron Spray Ionization Mass Spectrometry (ESI-MS) data (g/mol): $MW_{calcd.}$: 1177.7924; MW_{found}: 1177.8264.

The samples of TriTOAC4 and NR adsorbed on the SiO_2 (denoted correspondingly as TriTOAC4/SiO_2 and NR/SiO_2) were prepared as following. The SiO_2 powders were put on the surface of a 0.1 μm Amicon Ultrafree-MC Durapore PVDF centrifugal filter (Millipore, MA, USA). Then, methanol solutions of TriTOAC4 or NR were added and the system was left for 30 min at room temperature. Then, a centrifugation (2000 rpm, 4 min, 25 °C) was performed to remove the solution with the non-adsorbed molecules. The samples were dried on filters in an argon stream and put into 3-mm glass tubes. Finally, air was pumped out (10^{-3} torr) and tubes were sealed.

2.2. EPR/ESE measurements

The measurements of continuous wave EPR spectra, ESE decays and echo-detected (ED) EPR spectra were carried out on an X-band ELEXSYS E580 9-GHz FT-EPR spectrometer (Bruker, Bremen, Germany) equipped with a split-ring Bruker ER 4118X-MS3 resonator inside an CF 935 cryostat (Oxford Instruments, Abingdon, UK). The temperature was controlled by a nitrogen stream with an accuracy of ±0.5 K. In ESE experiments, the resonator cavity was overcoupled to provide a ringing time of about 100 ns. The ESE measurements were performed by microwave two- (90°–τ–180°–τ–*echo*) and three-pulse (90°–τ–90°–*T*–90°–τ–*echo*) sequences. The pulse lengths were 16 ns and 32 ns for 90°- and 180°-pulses, respectively. In all cases the time delay τ was scanned, changing from 120 ns with steps of 4 ns. The ED EPR spectra were obtained as an echo signal amplitude with the time delay τ kept constant (and in the three-pulse experiments the time interval *T* constant as well) and the magnetic field scanned.

3. Results

The measurements were carried out in the temperature range of 80–295 K. The CW spectra (not shown) in the whole temperature range studied were typical for immobilized nitroxides diluted in matrix and did not show an extra line broadening typical for their aggregation. An example of ED EPR spectra obtained at 100 K and 250 K (for the TriTOAC4/SiO_2 sample) with different time delays τ (120, 300, and 600 ns) is shown in Fig. 1. These spectra are

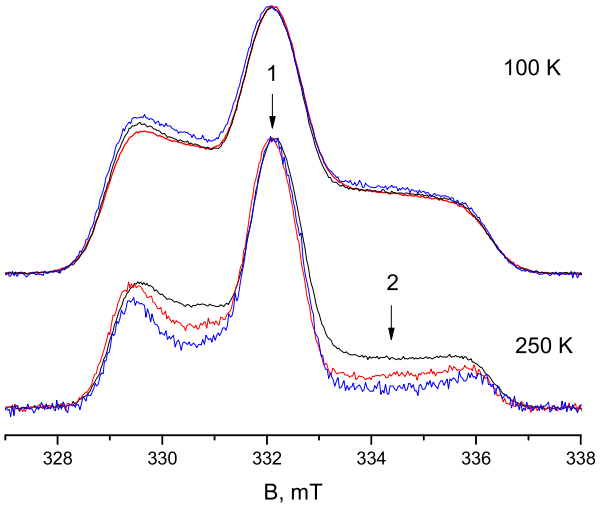

Fig. 1. ED EPR spectra obtained with a two-pulse microwave sequence, with τ fixed to 120 ns (black line), 300 ns (red line), and 600 ns (blue line), on the sample TriTOAC4/SiO_2 at the two temperatures indicated. Two spectral positions possessing the smallest (1) and largest (2) anisotropies are also shown.

normalized by the central peak amplitude (the field position 1 in Fig. 1). This normalization allows to exclude all field-independent spin-relaxation mechanisms.

From Fig. 1 one can see that at 250 K all spectral positions with increasing τ are decreasing with respect to the spectral maximum. This effect implies a faster spin relaxation at these positions. In the center of the high-field component (the field position 2 in Fig. 1) the decrease is most pronounced. Meanwhile, the relaxation of the two outer spectral shoulders is relatively slower. This behavior is in full agreement with the model of stochastic molecular librations [1–3,10–13]. To illustrate this behavior, for a nitroxide solid-state EPR let us consider an approximation of axial anisotropy of the g- and hyperfine interaction (HFI) tensors, with the parallel and perpendicular principal values of the g- and HFI tensors denoted as $g_{||}$, $g_{\perp}$, $A_{||}$, $A_{\perp}$. In the case of rotation around the X molecular axis by a small angle $\alpha(t)$, the resonance frequency deviates by a small value $\Delta\omega(t)$ [1–4,13]:

$$\Delta\omega(t) \cong \alpha(t)R_x(\theta,\varphi) \quad (1)$$

where

$$R_x(\theta,\phi) = \gamma[B(g_{\perp}-g_{||}) + \frac{m(A_{\perp}^2 - A_{||}^2)}{(A_{\perp}\sin^2\theta + A_{||}^2\cos^2\theta)^{1/2}}]\cos\theta\sin\theta\sin\varphi,$$

with the angles θ and φ determining the orientation of the magnetic field **B** in the molecular frame and m being the nitrogen nuclear spin projection onto its quantization axis. For small-angle motions, angles θ and φ may be considered as constants, as well as the m value, the latter because of the low rate of nitrogen spin flips in solids. For a motion around the Y molecular axis, sin φ in (1) is to be replaced by cos φ. For a motion around the Z molecular axis under the used axial approximation, $\Delta\omega(t) = 0$. One can see from Eq. (1) that for $m = 0$ (central HFI component) and for canonical orientations, for which $\theta = \pi/2$ (two spectral shoulders), the relaxation is indeed expected to be slower than for other spectral positions. Note that two other canonical orientations in the spectrum corresponding to $\theta = \pi/2$ are too close to the large central peak and therefore they are not seen.

Fig. 1 shows that at 100 K these effects are suppressed. This observation may be readily assigned to freezing of the motions. Moreover, for $\tau = 600$ ns the side components at 100 K become somewhat larger. This behavior may be easily explained by the field-dependent relaxation induced by dipole-dipole interactions between electron spins (the so-called effect of "instantaneous diffusion" in ESE formation which is induced by microwave pulse perturbation of the dipolar-coupled spin system – see for details e.g. [11]). These interactions result in a faster relaxation for the most intense component.

Fig. 2 shows how the ED EPR spectra change with increasing temperature (with the time delay τ kept constant). One can see that these variations qualitatively look similar to those with increasing τ (Fig. 1): the side components are also diminishing, and the canonical orientations relax slower.

The alternative ways to present the ESE experimental data on motion-induced spin relaxation are temporal decays. To exclude field-independent relaxation processes, a comparison of the echo decays in the most isotropic and the most anisotropic field positions (in Fig. 1 see positions 1 and 2, respectively) allows refining the pure contribution of the orientational motions. A semi-logarithmic plot of the echo decays in these two field positions, $E_1(2\tau)$ and $E_2(2\tau)$, and of their ratio, $E_2(2\tau)/E_1(2\tau)$, is given in Fig. 3. This ratio can be well approximated by a straight line (in the time range of 0.24–0.92 μs), which implies an exponential decay. The exponentiality of the decay is indeed predicted by theoretical consideration of stochastic molecular libration model [1–3,10–13].

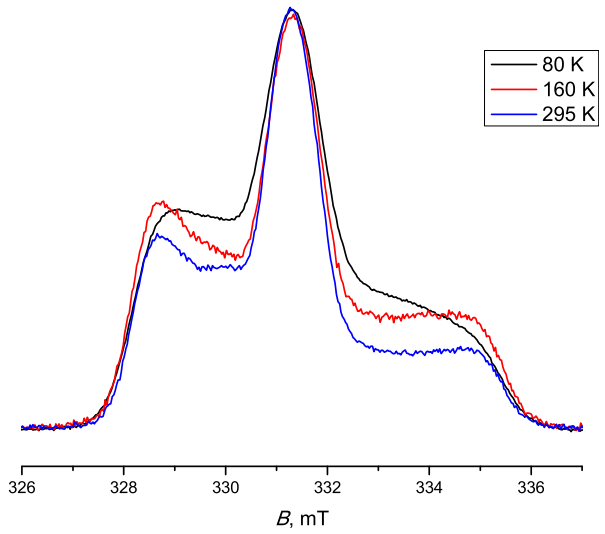

Fig. 2. ED-EPR spectra for TriTOAC4/SiO_2 sample at different temperatures. The time delay τ is 120 ns in all cases.

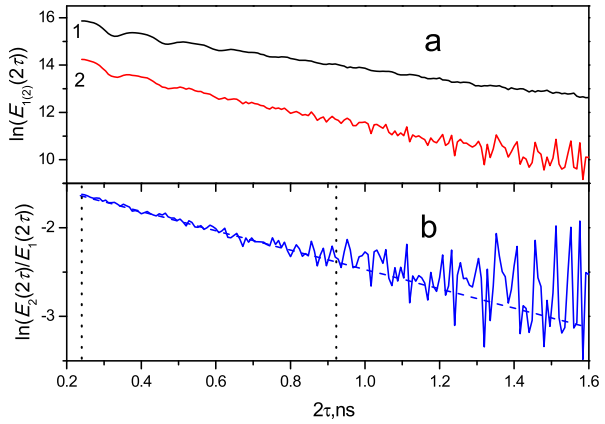

Fig. 3. Semi-logarithmic plot for (a) ESE decays for the field positions 1 and 2 (see Fig. 1) and (b) for the ratio of these decays, with the linear approximation shown (dashed line). The approximation was obtained by fitting in the time range embraced by the vertical dotted lines; the tangent of the slope angle provides the ΔW value. The sample is TriTOAC4/SiO_2 at 240 K.

Fast motions imply the applicability of the Redfield's theory of spin relaxation, $<\Delta\omega^2>\ \tau_c^2 \ll 1$, where τ_c is the correlation time for the motion. In that case, the rate of the exponential echo decay, W, is given by

$$W = <\Delta\omega^2(t)>\tau_c = R_x^2(\theta,\varphi)\alpha^2(t)\tau_c \quad (2)$$

As this relaxation appears because of the spectral anisotropy, it is natural to call it anisotropic relaxation.

For the comparative two-pulse ESE experiment described above, in which the echo decay is taken at two field positions and then divided by each other, we have

$$E(2\tau) \equiv E_2(2\tau)/E_1(2\tau) = const\ \exp(-2\tau\Delta W) \quad (3)$$

where ΔW is difference of the relaxation rates for these two positions. The ΔW value may be directly measured as a tangent of the slope angle in Fig. 3b.

Note that the spectral simulations performed within the Redfield' theory for the two employed spectral positions in the simulated EPR spectrum [13] have shown that

$$\Delta W = K < \alpha^2 > \tau_c, \quad (4)$$

where $\langle\alpha^2\rangle$ is the mean angular amplitude and K is a numerical coefficient, equal approximately to 10^{17} rad^{-2} s^{-2} [13], with the exact value depending on the magnetic parameters of the used nitroxide spin label.

Fig. 4 shows the semi-logarithmic plot of the $E_2(2\tau)/E_1(2\tau)$ representative data obtained for different temperatures. These data, like those shown in Fig. 3b, also may be approximated fairly well by straight lines. The line slope becomes more negative with temperature increase, which indicates a ΔW increase. Note that a slightly positive slope at 80 K may be explained by the aforementioned field-dependent relaxation induced by "instantaneous diffusion", which is also known to decay exponentially [11]. As the dipole-dipole contribution to the ESE decay is temperature-independent, the ΔW value at any temperature is to be subtracted by those obtained at 80–100 K, where motions are not expected to be active.

Meanwhile, basing on the theory of the "instantaneous diffusion" mechanism, the positive slope at 80 K allows to estimate the surface concentration of the adsorbed molecules. As spin labels on surface are expected to have a two-dimensional spatial distribution, the approximating formula derived for this mechanism may be employed [40]:

$$E_{inst.diff.}(\tau) \cong E_0 \exp(-3.21\,\sigma p (g^2\mu_B^2\tau/\hbar)^{\frac{2}{3}}) \quad (5)$$

where σ is the surface density in cm^{-2} units, g is the g-factor, μ_B is the Bohr magneton, and the dimensionless parameter p reflex the efficiency of the pulse excitation. Data in Fig. 4 for 80 K may be well approximated by the $\tau^{\frac{2}{3}}$ temporal dependence (data not given), and application of Eq. (5), with p taken as 0.2 [40], then readily provides $\sigma \approx 7\ 10^{11}$ cm^{-2}. This σ value in turn allows to estimate the distance between the molecules on the surface as ~10 nm. This distance is much larger than the molecular sizes for the both adsorbed molecules used, so these molecules indeed are diluted on the surface.

The time range for the linear approximation (see vertical dotted lines in Figs. 3b and 4) was taken the same for all temperatures and all samples. The temperature dependences of the ΔW anisotropic relaxation rate for all the samples studied are shown in Fig. 5 (above 300 K the ESE signal decayed too fast). The ΔW values are almost zero below ~130 K, but exhibit an increase with temperature up to about 250 ± 10 K. The maximum ΔW_{max} value for the NR/SiO$_2$ sample is 1.48 ± 0.05 μs^{-1} and for the TriTOAC4/SiO$_2$ sample is 1.04 ± 0.05 μs^{-1}. Above ~250 K both dependences in Fig. 5 show a slight decrease.

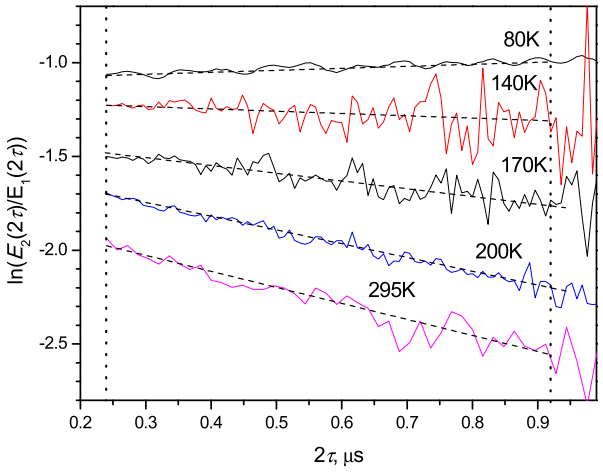

Fig. 4. The same as in Fig. 3b, for other selected temperatures. Data are shifted along the vertical axis for convenience.

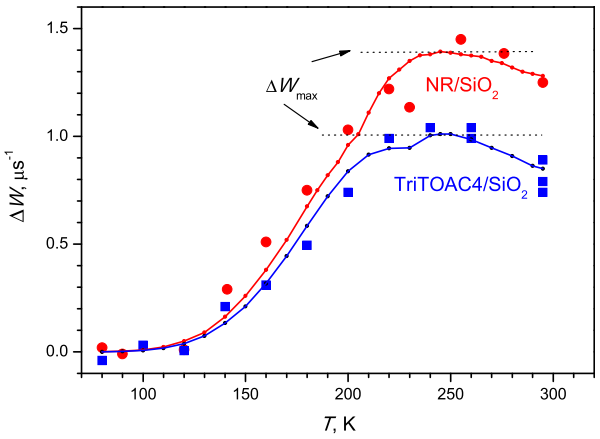

Fig. 5. Temperature dependence of the anisotropic relaxation rate ΔW for the samples TriTOAC4/SiO$_2$ (squares) and NR/SiO$_2$ (circles). Solid curves: simulation using Eq. (6) with τ_c = 65 ns and $\alpha = \exp(-1.94 - 529\ \mathrm{K}/T)$ for the NR/SiO$_2$ sample, and with τ_c = 40 ns and $\alpha = \exp(-1.68 - 523\ \mathrm{K}/T)$ for the TriTOAC4/SiO$_2$ sample. Two horizontal dashed lines show the attained maximal ΔW_{max} values.

In our simulations we used a simple model of random jumps around an axis lying in the xy plane of the nitroxide molecular frame by an angle ± α. ESE decays in this model are described by the formula [41]

$$E(2\tau) = const\left[\left(chR\tau + \frac{w}{R}shR\tau\right)^2 - \frac{\Delta\omega^2}{4R^2}sh^2R\tau\right]e^{-2w\tau} \quad (6)$$

where $w = \frac{1}{2\tau_c}$ and $R^2 = w^2 - \frac{\Delta\omega^2}{4}$.

One can found that in the case of fast motion, $\langle\Delta\omega^2\rangle\ \tau_c^2 \ll 1$, when also $\tau \gg \tau_c$, Eq. (6) is reduced to the exponential dependence, $E(2\tau) = \exp(-2\tau\Delta\omega^2\tau_c)$, that is in full agreement with Eq. (2). The advantage of this model is however its applicability to any $\Delta\omega^2\tau_c^2$ value, *i. e.* this model is not restricted by the condition of fast motion underlying the Redfield's theory of spin relaxation.

The ED EPR spectra were simulated as described in detail elsewhere [11]. The hyperfine interaction and g-tensor parameters were evaluated from the obtained CW EPR spectra. The results of the simulations are presented in Fig. 6. In the calculations only two input parameters, τ_c and α, were varied.

The calculated curves in Fig. 6 at small α are linear and coincide well with the predictions of Eqs. (3) and (4), just as it was expected within the Redfield's theory. The parameter K in Eq. (4) was found to be equal to 1.9 10^{17} rad^{-2} s^{-2}. At larger α, the curves become essentially non-linear. This result may be related to a violation of the $\langle\Delta\omega^2\rangle\ \tau_c^2 \ll 1$ condition for the Redfield's theory validity. Indeed, for τ_c = 40 ns, Fig. 6 shows that the linearity is distorted when $\alpha \approx 0.02$ rad. Using Eqs. (2) and (4), one obtains that $\langle\Delta\omega^2\rangle \approx K\alpha^2$, so the linearity is distorted when $\langle\Delta\omega^2\rangle\ \tau_c^2 \approx 0.1$.

However in the time window of the ESE experiment shown in Fig. 6 by two vertical dotted lines, the calculated curves may be approximated by straight lines, with an effective slope ΔW_{eff}. One can see that the ΔW_{eff} value with varying α at a given τ_c attains its maximal value, ΔW_{max}. These values are plotted in Fig. 7 as a function of τ_c. A comparison of the calculated data given in Fig. 7 with the ΔW_{max} values found in the experiments (Fig. 5) allows one to estimate the angles of reorientation α and the correlation time τ_c at the temperature where the maximum is achieved (250 K). We found that for the NR/SiO$_2$ sample $\alpha \approx 0.02$ rad and $\tau_c \approx 65$ ns, while for the TriTOAC4/SiO$_2$ sample $\alpha \approx 0.02$ rad and $\tau_c \approx 40$ ns.

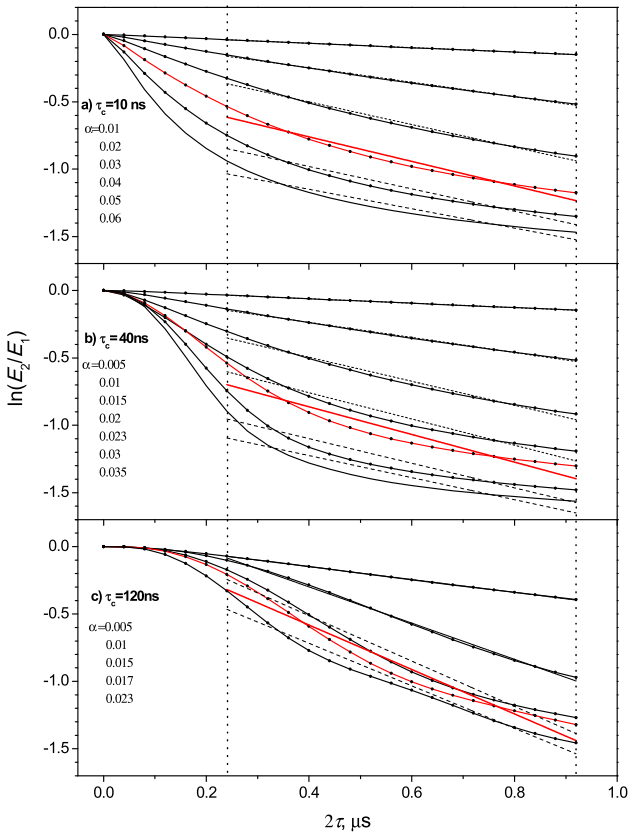

Fig 6. Simulations of the ratio of echo decays for spectral positions 1 and 2 (see Fig. 1), within the two-site jump model (Eq. (6)). Data are presented in a semi-logarithmic plot (cf. Fig. 3b and 4) for three correlation times and different angles α indicated in the order of the initial slope increase. The dashed straight lines are linear approximation within the time interval encompasses by the vertical dotted lines (cf. Fig. 3b and 4); the solid straight lines indicate the maximal slope attained for the τ_c employed.

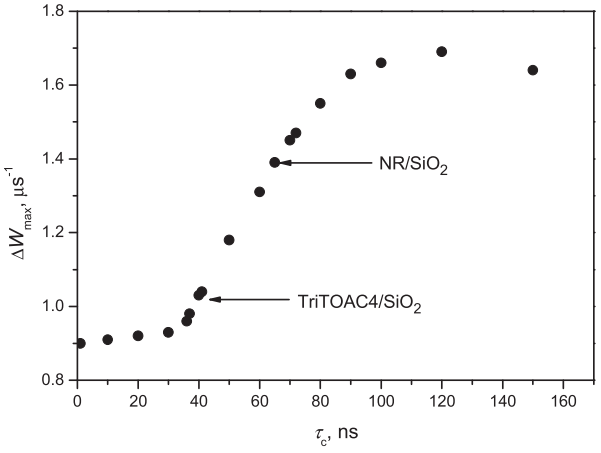

Fig. 7. Calculated correlation time dependence of the maximal anisotropic relaxation rate, within the two-site jump model. Two horizontal arrows indicate the two experimental situations reported in Fig. 5.

Fig. 8 shows a comparison of the ED-EPR spectra obtained with the two-pulse ($2\tau = 0.24$ μs) and the three-pulse ($2\tau = 0.24$ μs, $T = 2$ μs) microwave sequences at room temperature. Clearly, these two spectra coincide with good accuracy. This result implies that τ_c is indeed lying in the nanosecond time scale, because stimulated echo is influenced by motion only when the time interval T is smaller than or comparable to τ_c [13,42].

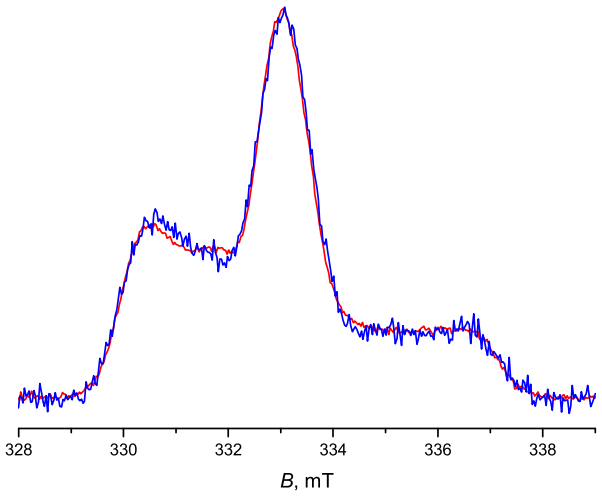

Fig. 8. ED EPR spectra of the sample TriTOAC4/SiO_2 obtained at room temperature with the two-pulse microwave sequence ($2\tau = 0.24$ μs) (smooth line) and the three-pulse microwave sequence ($2\tau = 0.24$ μs, $T = 2$ μs) (noisy line), normalized to the central peak.

4. Discussion

The experimental results obtained in this work for adsorbed molecules refer to their individual motions because of the dilution conditions on the surface. Also, the solid inorganic matrix does not participate in the motion. For both NR and TriTOAC4 molecules adsorbed on the SiO_2 surface, the ΔW temperature dependence shows a saturating behavior – see Fig. 5. This behavior is reproduced in simulations within a simple two-site jump model (Figs. 5 and 6) in which motion by the angles $\pm\alpha$ around a given axis is assumed. Qualitatively saturating behavior may be explained by breakdown of the conditions of fast motion imposed by the Redfield's theory, $\Delta\omega^2\tau_c^2 << 1$, which takes place when the libration angle α reaches a critical magnitude.

A comparison of the calculated and experimental maximal ΔW_{max} values allows to assess both the librational angle α and the correlation time τ_c – at the temperature where this maximum is achieved (~250 K). Data in Fig. 7 show that τ_c is of the order of several tens of nanoseconds and the angle α is around 0.02 rad (*i.e.* about 1°).

Fig. 5 shows also the simulations of the ΔW temperature dependence under the approximation of a constant correlation time τ_c and an Arrhenius behavior of the angle α, $\alpha = \exp(p - E/T)$ rad (like it was previously assumed in references [12,43]). As τ_c is expected to decrease with increasing temperature, the observed saturation takes place if the angle α increases with temperature faster than τ_c decreases. The best-fitted p and E values were found to be respectively −1.68 and 523 K for the TriTOAC4/SiO_2 sample, and −1.60 and 532 K for the NR/SiO_2 sample. One can see from Fig. 5 a rather good agreement between these simulations and the experiment; some non-smoothness of the calculated curves is related with the simplicity of the two-site jump model employed.

It would be interesting to compare the obtained results with the analogous data found for biological media, where cooperative effects may appear. This comparison is presented in Fig. 9, where the data are given for TriTOAC1 (where the TOAC residue replaces Aib at position 1 of the trichogin structure) embedded in DPPC (1,2-dipalmitoylphosphatidylcholine) and POPC (1-palmitoyl-2-oleoylphosphatidylcholine) lipid bilayers [43], and for spin-labeled lysozyme [44]. One can see from data in Fig. 9 that ESE-detected stochastic librations appear in biological systems either above 100 K or above 130 K. Note that this onset of motions is not likely

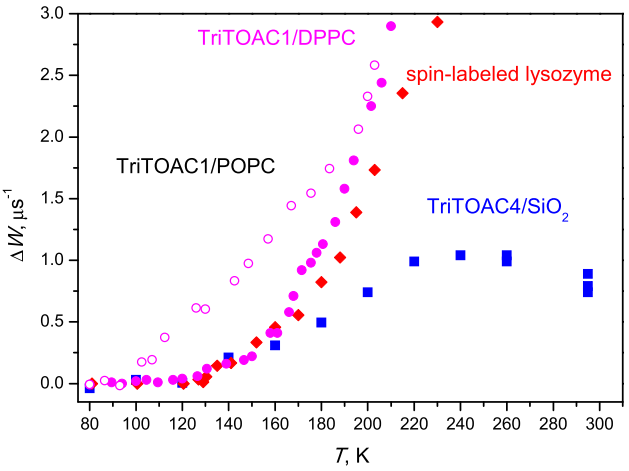

Fig. 9. Comparison of data for the TriTOAC4/SiO_2 sample (squares, the same as in Fig. 5) with the analogous data published for spin-labeled lysozyme [44] (rhombs), for spin-labeled peptides in DPPC bilayers [43] (filled circles) and in POPC bilayers [43] (open circles).

because of the internal flexibility of the molecules. Indeed, stochastic librations detected for nitroxide spin labels at X-band are known to strongly depend on the matrix and not depend on the molecular structure (see Ref. [45] and also below).

It is interesting to note that numerous data accumulated in literature also evidence that ESE-detected stochastic librations appear, depending on the system, either above 100 K or above 130 K. Onset of the motions above 100 K was found for spin-labeled stearic acids interacting with membranous Na,K-ATPase [18], for spin-labeled phospholipids in DPPC/Cholesterol (50:50 mol%) bilayer [10], for antimicrobial peptide alamethicin spin-labeled in the middle of the amino-acid chain and near its C-terminus [17], for spin probe in dry lysozyme [44], for frozen ionic liquids [26,27] (here motions appear between 80 and 100 K), and for spin-labeled molecules in POPC [15,43] and DOPC (dioleoyl-*glycero*-phosphocholine) [15] bilayers.

Onset of the motions above 130 K was found for spin-labeled molecules in DHPC [12] and DPPC bilayers [43], for antimicrobial peptide alamethicin spin-labeled near its N-terminus [17], for hydrated spin-labeled lysozyme [44].

Meanwhile for spin probes in simple molecular glass-formers, ESE study showed that the onset of stochastic librations corresponds to their glass transition temperatures [44–46]. Note that at the high-field W-band EPR the motions of spin probes in *ortho*-terphenyl (glass transition temperature 243 K) become visible already above ~130 K [31]. This result may be explained by the higher orientational sensitivity in the W-band, so that the intramolecular motions contribute here to the ESE decays [31].

For biological systems the temperatures of 100 and 130 K of the onset of the motion hardly can be related with their glass transition. To date, the nature of these temperature points remains unknown. We mention only that the onset of motions at 100 K occurs for the systems nanoscopically more disordered, as compared with the systems where this onset occurs at 130 K – like it takes place for the POPC bilayer as compared to the DPPC bilayer (Fig. 9).

Fig. 9 for lysozyme and for DPPC bilayers shows an enhancing relaxation above ~160–180 K, in comparison with the case of individual motion on the surface. This enhancement indicates that different channels of motion-induced spin relaxation appear which work in a multiplicative way; most probably these relaxation channels are indeed related with the cooperative motion. Fig. 9 also shows that cooperative motions may result in a ΔW rate much higher than that found for individual motions of adsorbed molecules (so that above 160–180 K cooperative motions dominate). Meanwhile, for motion starting at 100 K (Fig. 9), the cooperative motions probably appear even at this temperature.

We propose that for any molecular system the onset of motional cooperativity may be detected as an excess of the measured ΔW rate over the 1 μs^{-1} value found here for the adsorbed molecules (see Fig. 9), for the experimental setup employed.

And finally, note that onset of motion near 130 K in biological media was also observed in neutron scattering experiments [47–50]. This finding was explained as the onset of methyl group rotations. The data treatment used in the present work, however, excludes the methyl group rotation contribution to the echo decays [44]. Therefore, the observed effects in neutron scattering [47–50] also may be attributed to the individual motion of the molecules in their entrapping molecular cages, because of the closeness of the experimental time window – nanoseconds for both the ESE-detected stochastic librations and for the mean-squared displacements detected in neutron scattering.

5. Conclusions

Molecules adsorbed at low concentration on a solid surface possess only negligible mutual interactions. Therefore, possible cooperativity in their motion may be certainly ruled out. This is why an ESE study of spin-labeled molecules on the surface allows extraction of the pure effects of individual stochastic molecular librations. The temperature dependence of anisotropic relaxation rate ΔW obtained here demonstrates a saturating behavior. This feature was reproduced in simulations based on a simple model of jumps between two orientations by an angles $\pm\alpha$. The saturation in this model is explained as a consequence that the libration angle α reaches its critical value for a given correlation time τ_c so that the condition of the Redfield's theory applicability, $\Delta\omega^2\tau_c^2 << 1$, is violated. Comparison with experiment allowed to estimate that near the saturation (at ~250 K) τ_c is of the order of several tens of nanoseconds and the angle α is around 0.02 rad.

This saturating behavior may be considered as an exclusive property of the molecular individual motions. The maximal anisotropic relaxation rate attained in this case, ΔW_{max}, is close to the value of 1 μs^{-1} (in the experimental setup used). As in this work for two very different molecules – a small highly-polar nitroxide radical and a large spin-labeled peptide – quite similar ΔW temperature dependences were found, the effect seems to be independent on the nature of the molecules. We suppose that for any molecular system an excess of the spin relaxation rate above this maximal value may be ascribed to the effects of cooperative motions. Note that this maximal value was obtained in experiment; the theoretical two-site model was employed only to explain the observed saturating temperature behavior.

This excess implies that motion occurs not only around a particular single molecular axis but it rather involves independent reorientations around several axes. Comparison with literature data on biological and molecular systems of different origin has shown that effects of cooperativity indeed are important and even may dominate. The onset of cooperative motions certainly takes place in frozen biological media for temperatures above 160–180 K.

Declaration of Competing Interest

The authors declared that there is no conflict of interest.

Acknowledgements

Authors are thankful to Dr. I. A. Kirilyuk of Novosibirsk Institute of Organic Chemistry of Russian Academy of Sciences for donating

the NR. This work was supported by the Russian Science Foundation, project No. 15-15-00021.

References

[1] S.A. Dzuba, Yu.D. Tsvetkov, A.G. Maryasov, Echo-induced EPR spectra of nitroxides in organic glasses: model of molecular orientational motion near equilibrium position, Chem. Phys. Lett. 188 (1992) 217.

[2] S.A. Dzuba, Librational motion of guest spin probe molecules in glassy media, Phys. Lett. A 213 (1996) 77–84.

[3] E.P. Kirilina, S.A. Dzuba, A.G. Maryasov, Yu.D. Tsvetkov, Librational dynamics of nitroxide molecules in a molecular glass studied by echo-detected EPR, Appl. Magn. Reson. 21 (2001) 203–221.

[4] E.P. Kirilina, T.F. Prisner, M. Bennati, B. Endeward, S.A. Dzuba, M.R. Fuchs, K. Möbius, A. Schnegg, Molecular dynamics of nitroxides in glasses as studied by multifrequency EPR, Magn. Reson. Chem. 43 (2005) S119–S129.

[5] M.M. Hertel, V.P. Denysenkov, M. Bennati, T.F. Prisner, Pulsed 180-GHz EPR/ENDOR/PELDOR spectroscopy, Magn. Reson. Chem. 43 (2005) S248–S255.

[6] M. Rohrer, P. Gast, K. Möbius, T.F. Prisner, Anisotropic motion of semiquinones in photosynthetic reaction centers of *Rhodobacter sphaeroides* R26 and in frozen isopropanol solution as measured by pulsed high-field EPR at 95 GHz, Chem. Phys. Lett. 259 (1996) 523–530.

[7] A. Schnegg, M. Fuhs, M. Rohrer, W. Lubitz, T.F. Prisner, K. Möbius, Molecular dynamics of Q_A^- and Q_B^- in photosynthetic bacterial reaction centers studied by pulsed high-field EPR at 95 GHz, J. Phys. Chem. B 106 (2002) 9454–9462.

[8] A. Savitsky, K. Möbius, High-field EPR, Photosynth. Res. 102 (2009) 311–333.

[9] I.V. Borovykh, P. Gast, S.A. Dzuba, The dynamical transition in proteins of bacterial photosynthetic reaction centers observed by echo-detected EPR of specific spin labels, Appl. Magn. Reson. 31 (2007) 159–166.

[10] D.A. Erilov, R. Bartucci, R. Guzzi, D. Marsh, S.A. Dzuba, L. Sportelli, Librational motion of spin-labeled lipids in high-cholesterol containing membranes from echo-detected EPR spectra, Biophys. J. 87 (2004) 3873–3881.

[11] D.A. Erilov, R. Bartucci, R. Guzzi, D. Marsh, S.A. Dzuba, L. Sportelli, Echo-detected electron paramagnetic resonance spectra of spin-labeled lipids in membrane model systems, J. Phys. Chem. B 108 (2004) 4501–4507.

[12] E. Aloi, M. Oranges, R. Guzzi, R. Bartucci, Low-temperature dynamics of chain-labeled lipids in ester- and ether-linked phosphatidylcholine membranes, J. Phys. Chem. B 121 (2017) 9239–9246.

[13] N.P. Isaev, S.A. Dzuba, Fast stochastic librations and slow rotations of spin labeled stearic acids in a model phospholipid bilayer at cryogenic temperatures, J. Phys. Chem. B 112 (2008) 13285–13291.

[14] K.B. Konov, N.P. Isaev, S.A. Dzuba, Low-temperature molecular motions in lipid bilayers in the presence of sugars: insights into cryoprotective mechanisms, J. Phys. Chem. B 118 (2014) 12478–12485.

[15] E. Aloi, R. Guzzi, R. Bartucci, Unsaturated lipid bilayers at cryogenic temperature: librational dynamics of chain-labeled lipids from pulsed and CW-EPR, Phys. Chem. Chem. Phys. 21 (2019) 18699–18705.

[16] F. De Simone, R. Guzzi, L. Sportelli, D. Marsh, R. Bartucci, Electron spin-echo studies of spin-labelled lipid membranes and free fatty acids interacting with human serum albumin, Biochim. Biophys. Acta 1768 (2007) 1541–1549.

[17] R. Bartucci, R. Guzzi, M. De Zotti, C. Toniolo, L. Sportelli, D. Marsh, Backbone dynamics of alamethicin bound to lipid membranes: spin-echo electron paramagnetic resonance of TOAC spin-labels, Biophys. J. 94 (2008) 2698–2705.

[18] R. Guzzi, R. Bartucci, M. Esmann, D. Marsh, Lipid librations at the interface with the Na, K-ATPase, Biophys. J. 108 (2015) 2825–2832.

[19] R. Guzzi, M. Babavali, R. Bartucci, L. Sportelli, M. Esmann, D. Marsh, Spin-echo EPR of Na, K-ATPase unfolding by urea, Biochim. Biophys. Acta 2011 (1808) 1618–1628.

[20] F. Scarpelli, R. Bartucci, L. Sportelli, R. Guzzi, Solvent effect on librational dynamics of spin-labelled haemoglobin by ED- and CW-EPR, Eur. Biophys. J. 40 (2011) 273.

[21] H.-J. Steinhoff, A. Savitsky, C. Wegener, M. Pfeiffer, M. Plato, K. Möbius, High-field EPR studies of the structure and conformational changes of site-directed spin labeled bacteriorhodopsin, Biochim. Biophys. Acta 1457 (2000) 253–262.

[22] A. Volkov, C. Dockter, T. Bund, H. Paulsen, G. Jeschke, Pulsed EPR determination of water accessibility to spin-labeled amino acid residues in LHCIIbA, Biophys. J. 96 (2009) 1124–1141.

[23] V.S. Oganesyan, A general approach for prediction of motional EPR spectra from Molecular Dynamics (MD) simulations: application to spin labelled protein, Phys. Chem. Chem. Phys. 13 (2011) 4724–4737.

[24] S.A. Dzuba, Y.A. Golovina, Yu.D. Tsvetkov, Echo-induced EPR spectra of spin probes as a method for identification of glassy state in biological objects, J. Magn. Reson. B 101 (1993) 134–138.

[25] D. Leporini, G. Jeschke, Cage effects on the librational motion in ionomeric homopolymers and block copolymers, Phil. Mag. 84 (2004) 1567–1572.

[26] M.Y. Ivanov, O.A. Krumkacheva, S.A. Dzuba, M.V. Fedin, Microscopic rigidity and heterogeneity of ionic liquids probed by stochastic molecular librations of the dissolved nitroxides, Phys. Chem. Chem. Phys. 19 (2017) 26158–26163.

[27] M.Y. Ivanov, S.A. Prikhod'ko, N.Y. Adonin, I.A. Kirilyuk, S.V. Adichtchev, N.V. Surovtsev, S.A. Dzuba, M.V. Fedin, Structural anomalies in ionic liquids near the glass transition revealed by pulse, EPR, J. Phys. Chem. Lett. 9 (2018) 4607–4612.

[28] A.A. Kuzhelev, O.A. Krumkacheva, M.Y. Ivanov, S.A. Prikhod'ko, N.Y. Adonin, V. M. Tormyshev, M.K. Bowman, M.V. Fedin, E.G. Bagryanskaya, Pulse EPR of triarylmethyl probes: a new approach for the investigation of molecular motions in soft matter, J. Phys. Chem. B 122 (2018) 8624–8630.

[29] E.G. Bagryanskaya, D.N. Polovyanenko, M.V. Fedin, L. Kulik, A. Schnegg, A. Savitsky, K. Möbius, A.W. Coleman, G.S. Ananchenko, J.A. Ripmeester, Multifrequency EPR study of the mobility of nitroxides in solid-state calixarene nanocapsules, Phys. Chem. Chem. Phys. 11 (2009) 6700–6707.

[30] N.P. Isaev, M.V. Fedin, S.A. Dzuba, X- and Q-band electron spin echo study of stochastic molecular librations of spin labels in lipid bilayers, Appl. Magn. Reson. 44 (2013) 133–142.

[31] A. Savitsky, M. Plato, K. Möbius, The temperature dependence of nitroxide spin–label interaction parameters: a high-field EPR study of intramolecular motional contributions, Appl. Magn. Reson. 37 (2010) 415–434.

[32] A. Barbon, M. Bortolus, M. Brustolon, A. Comotti, A.L. Maniero, U. Segre, P. Sozzani, Dynamics of the triplet state of a dithiophene in different solid matrixes studied by transient and pulse EPR techniques, J. Phys. Chem. B 107 (2003) 3325–3331.

[33] M.Y. Ivanov, S.L. Veber, S.A. Prikhod'ko, N.Y. Adonin, E.G. Bagryanskaya, M.V. Fedin, Probing microenvironment in ionic liquids by time-resolved EPR of photoexcited triplets, J. Phys. Chem. B 119 (2015) 13440–13449.

[34] S.V. Paschenko, Yu.V. Toropov, S.A. Dzuba, Yu.D. Tsvetkov, A.Kh. Vorobiev, Temperature dependence of amplitudes of libration motion of guest spin probe molecules in organic glasses, J. Chem. Phys. 110 (1999) 8150–8154.

[35] D.A. Chernova, A.K. Vorobiev, Molecular mobility of nitroxide spin probes in glassy polymers. Quasi-libration model, J. Polym. Sci., Part B: Polym. Phys. 47 (2009) 107–120.

[36] , J. Polym. Sci. Part B: Polym. Phys. 57 (13) (2019) 819–825, https://doi.org/10.1002/polb.v57.1310.1002/polb.24836.

[37] A.V. Bogdanov, A.Kh. Vorobiev, Orientation order and rotation mobility of nitroxide biradicals determined by quantitative simulation of EPR spectra, Phys. Chem. Chem. Phys. 18 (2016) 31144–31153.

[38] A.Kh. Vorobiev, A.V. Bogdanov, T.S. Yankova, N.A. Chumakova, Spin probe determination of molecular orientation distribution and rotational mobility in liquid crystals: model-free approach, J. Phys. Chem. B 123 (2019) 5875–5891.

[39] E.F. Afanasyeva, V.N. Syryamina, M. De Zotti, F. Formaggio, C. Toniolo, S.A. Dzuba, Peptide antibiotic trichogin in model membranes: Self-association and capture of fatty acids, Biochim. Biophys. Acta (Biomembranes) 2019 (1861) 524–531.

[40] M.E. Kardash, S.A. Dzuba, Lipid-mediated clusters of guest molecules in model membranes and their dissolving in presence of lipid rafts, J. Phys. Chem. B 121 (2017) 5209–5217.

[41] K.M. Salikhov, S.A. Dzuba, A.M. Raitsimring, The theory of electron spin echo signal decay resulting from dipole-dipole interactions between paramagnetic centers in solids, J. Magn. Reson. 42 (1981) 255.

[42] S.A. Dzuba, E.P. Kirilina, E.S. Salnikov, L.V. Kulik, Restricted orientational motion of nitroxides in molecular glasses: Direct estimation of the motional time scale basing on the comparative study of primary and stimulated electron spin echo decays, J. Chem. Phys. 122 (2005) 094702.

[43] E.A. Golysheva, M. De Zotti, C. Toniolo, F. Formaggio, S.A. Dzuba, Low-temperature dynamical transition in lipid bilayers detected by spin-label ESE spectroscopy, Appl. Magn. Reson. 49 (2018) 1369–1383.

[44] E.A. Golysheva, G.Y. Shevelev, S.A. Dzuba, Dynamical transition in molecular glasses and proteins observed by spin relaxation of nitroxide spin probes and labels, J. Chem. Phys. 147 (2017) 064501.

[45] E.P. Kirilina, I.A. Grigoriev, S.A. Dzuba, Orientational motion of nitroxides in molecular glasses: dependence on the chemical structure, on the molecular size of the probe, and on the type of the matrix, J. Chem. Phys. 121 (2004) 12465–12471.

[46] S.A. Dzuba, E.P. Kirilina, E.S. Salnikov, On the possible manifestation of harmonic-anharmonic dynamical transition in glassy media in electron paramagnetic resonance of nitroxide spin probes, J. Chem. Phys. 125 (2006) 054502.

[47] S. Magazù, F. Migliardo, A. Benedetto, B. Vertessy, Protein dynamics by neutron scattering: the protein dynamical transition and the fragile-to-strong dynamical crossover in hydrated lysozyme, Chem. Phys. 424 (2013) 26–31.

[48] A. Benedetto, Protein dynamics by neutron scattering, Biophys. Chem. 182 (2013) 16–22.

[49] E. Mamontov, H. O'Neill, Q. Zhang, Mean-squared atomic displacements in hydrated lysozyme, native and denatured, J. Biol. Phys. 36 (2010) 291–297.

[50] S. Khodadadi, A.P. Sokolov, Protein dynamics: from rattling in a cage to structural relaxation, Soft Matter 11 (2015) 4984–4998.